Effect of cation local structure on the physical properties of sulphonated polyurethane ionomers based on toluene diisocyanate

Y. Samuel Ding*, Richard A. Register, Chang-zheng Yang†, and Stuart L. Cooper‡

Department of Chemical Engineering, University of Wisconsin – Madison, Madison, WI 53706, USA

(Received 15 July 1988; accepted 25 September 1988)

A series of sulphonated polyurethane ionomers based on poly(tetramethylene oxide) of molecular weight 1000, neutralized with Ca^{2+}, Ni^{2+}, Zn^{2+}, Cd^{2+}, Cs^{+} and Eu^{3+} were examined by extended X-ray absorption fine structure (EXAFS) spectroscopy. The degree of local order shown by EXAFS correlates inversely with the strain at which stress crystallization begins, indicating that the cohesiveness of the ionic aggregates controls the large-strain behaviour of the materials by suppressing ion-hopping. Upon hydration, the materials lose their mechanical strength. The local structure in the Ca^{2+}-neutralized material is insensitive to hydration, while that in the Ni^{2+}-neutralized material changes dramatically.

(Keywords: ionomer; polyurethane ionomer; extended X-ray absorption fine structure spectroscopy; local structure; structure–property relationships)

INTRODUCTION

In the two preceding papers[1,2], we have characterized sulphonated polyurethane ionomers based on toluene diisocyanate (TDI) and either poly(tetramethylene oxide), poly(propylene oxide) or polybutadiene (PTMO, PPO, or PBD) polyols by their thermomechanical properties and small-angle X-ray scattering (SAXS) patterns. In this paper, we will restrict our attention to a subset of these materials, namely those based on PTMO-1000 (the M1 series of the previous two papers) and consider how changing the neutralizing cation affects the internal structure of the ionic aggregates. These aggregates serve as physical crosslinks, and therefore the mechanical properties, especially at high strains, may be expected to depend on their cohesiveness. In the previous SAXS studies[2], it was noted that casting a material from a solvent which produced a high electron density within the ionic aggregates also produced a material with superior mechanical properties. The inference was that the property enhancement was due to better order within the aggregates.

Because of the small size and imperfect packing of these ionic aggregates, diffraction techniques can reveal little regarding their structure. On the other hand, extended X-ray absorption fine structure (EXAFS) spectroscopy is a powerful technique for determining the local atomic environment about a specific atom, and has been profitably applied to numerous ionomers[3–13]. The EXAFS signal is a modulation of the X-ray absorption coefficient on the high energy side of an elemental absorption edge, and it contains information on the coordination shells surrounding that atom. The type and number of atoms in a shell, as well as the distance to and disorder within a shell, are all reflected in the EXAFS data. In a previous investigation of non-crystallizable carboxy-telechelic polyisoprenes[10], it was found that the strain hardening behaviour observed when the neutralizing cation was divalent nickel or calcium could be explained by the presence of a second coordination shell in the EXAFS data due to a well defined cation–cation distance. It was inferred that the higher degree of order present in these aggregates made them more cohesive, and therefore the stressed chains could not relax by 'ion-hopping', where ionic groups are transported between aggregates[14–16]. Ion-hopping was discussed previously[1] in explaining the poorer physical properties observed with Cs^{+} and Zn^{2+} cations relative to Ni^{2+} and Eu^{3+} cations.

Therefore, it is of interest to see whether the mechanical properties in the M1 series can be correlated with the degree of order within the ionic aggregates, as determined by EXAFS. As before, the first two characters in the sample code (M1) indicate that the polyol used was PTMO-1000, and the last two digits are the cation's chemical symbol. In addition, two of the materials were swollen with water. Water can plasticize the ionic aggregates, presumably resulting in a decrease in their cohesiveness. Early studies on ethylene–methacrylic acid ionomers showed that saturation with water destroys the ionomer SAXS peak[17], indicating that the aggregates dissociate at very high water contents. More recent studies on sulphonated polystyrene ionomers by Fourier transform infra-red (*FT*i.r.) spectroscopy[18] and EXAFS[9] have shown that water molecules effectively displace other ligands from the cation's first coordination shell.

* Present address: Baxter Healthcare Corporation, Round Lake, IL 60073, USA

† Present address: Department of Chemistry, Nanking University, People's Republic of China

‡ To whom correspondence should be addressed

0032-3861/89/071221-06$03.00

EXPERIMENTAL

The synthesis of the polyurethane ionomers was described previously[1]. Samples for the EXAFS experimens were prepared by spin-casting at 60°C from DMF solution, and the films stacked to obtain sufficient absorbance for a good signal-to-noise ratio. Due to poor solubility in DMF, M1Cs was cast from methanol at 20°C. Hydration of the M1Ca and M1Ni samples was achieved by immersion of the samples in distilled water at room temperature for 30 min. Approximately 10 min were required to achieve swelling equilibrium, judging by visual observation of the dimensions of the swollen films, which approximately doubled in linear dimension when swollen.

The transmission EXAFS spectra were collected at the Cornell High Energy Synchrotron Source (CHESS). Most of the samples were studied on station C-1, although the higher energy of the cadmium K-edge required the use of station C-2 for sample M1Cd. The M1Ca, M1Ni, M1Zn, and M1Cd materials were studied at their K-edges, while the L_3 absorption edge was used for M1Cs and M1Eu because of the prohibitively high energies of the K-edge. Data reduction followed a standard procedure of pre-edge and post-edge background removal, extraction of the EXAFS oscillations $\chi(k)$, Fourier transformation of $\chi(k)$ and finally application of an inverse transform to isolate the EXAFS contribution from a selected region in real space[19–21]. Most of the model compounds used herein have been discussed previously[10]. In addition, Eu_2O_3 (Alfa, 99.99%) was studied at the Eu L_3 edge. The Eu_2O_3 sample was prepared by grinding the material to a homogeneous powder with polyethylene, and compression-moulding the mixture at 150°C and 8000 MPa into a uniform disk.

RESULTS AND DISCUSSION

The absorption modulation which is the EXAFS signal arises because photoelectrons which are ejected by the absorbed X-rays can be backscattered by atoms coordinated to the absorbing atom. Superposition of the outgoing and backscattered electron waves gives rise to an interference pattern. The EXAFS signal $\chi(k)$, where k is the photoelectron wavevector, contains information on the number N_j and type of atoms in coordination shell j, the distance R_j to this shell, and the static and vibrational disorder of the shell, measured as the Debye–Waller factor σ_j. To convert the EXAFS signal from wavevector to real space, it is Fourier transformed, and the magnitude of the transform is termed the radial structure function, or RSF. Each non-artefact peak in the RSF represents a distinct coordination shell. The peak positions in the RSF are shifted slightly from the true shell distances by a phase shift ϕ_j that the photoelectron experiences in backscattering.

The EXAFS data were analysed with single-electron single-scattering theory[20]:

$$\chi(k)=\sum_j \frac{N_j\gamma_j}{kR_j^2} f_j(k)\sin[2kR_j+\phi_j(k)]\exp(-2k_j^2\sigma_j^2) \quad (1)$$

Here k is the wavevector defined as

$$k=(2\pi/h)[2m(E-E_0)]^{1/2},$$

where E is the incident X-ray energy, h is Planck's constant, and m is the mass of an electron. E_0 is approximately equal to the edge energy, but is allowed to vary slightly to provide the best fit to the data and to correct for any errors in energy calibration[22]. γ_j accounts for the amplitude reduction due to inelastic scattering, and is approximated as $\exp(-2R_j/\lambda_j)$, with λ_j defining a mean free path parameter for shell j. The λ_j are obtained from the EXAFS from model compounds of known crystal structure. In determining λ_j, it is important that the structure of the model compound be as similar as possible to that of the unknown. The functions $f_j(k)$ and $\phi_j(k)$ are the backscattering amplitude and phase-shift functions, respectively, which are characteristic of the types of atom in shell j and the absorbing atom. The calculations of Teo and Lee[22] were used throughout for these functions, except for slight modifications to accommodate experimental data from model compounds studied previously, as discussed by Pan[29]. The accuracies of the R_j and N_j determinations are often quoted[23,24] as 1% and 20%, respectively, although these values depend strongly on the quality of the data, both in signal-to-noise ratio and the breadth of the usable wavevector range. It should be noted that equation (1) strictly applies only when the outgoing electron wave has s-type symmetry; that is, when a K or L_1 edge is studied[21]. EXAFS from the L_2 and L_3 edges is more complicated, but can be modelled with an equation[21,22] similar to equation (1), but using a different set of phase functions ϕ_j, which have also been calculated theoretically by Teo and Lee[22].

An example of the fitting process is shown in *Figure 1*, for the M1Zn sample. *Figure 1a* shows the EXAFS data, expressed as $k^3\chi$ *versus* k. Multiplying the signal by k^3 roughly cancels the diminution of the wave amplitude with increasing k, so that the data is more uniformly emphasized during the regression fitting. The dashed line in *Figure 1c* represents the magnitude of the Fourier transform of *Figure 1a*, the RSF. A single peak is visible at approximately 1.7 Å*. Note that peaks below 1.5 Å are artefacts of imperfect background subtraction. The single peak is then isolated and backtransformed to yield the circles in *Figure 1b*. Because there is only one shell present here, the backtransformed data look very much like the untreated data in *Figure 1a*. If multiple shells were present, the untreated data would be a composite of several damped sinusoids, thus necessitating Fourier filtering. A good fit to the backtransformed $k^3\chi$ data was achieved with approximately five oxygen atoms at a distance of 2.01 Å; the fit is shown as the solid line in *Figure 1b*. The calculated RSF is shown as the solid line in *Figure 1c*, and as can be seen it too fits the data well in the region of interest.

The EXAFS data, $k^3\chi$ and RSF, for each of the other samples is shown in *Figures 2–6*. Note the differences in scale between the figures. In *Figures 5* and *6*, the solid curves are for the dry and the dashed curves for the hydrated samples. Several points may be gleaned simply by observation of the RSFs. Consider first the dry samples. Widely varying degrees of order can be observed in the RSFs, with M1Ni and M1Eu exhibiting strong first shell peaks and small second shell peaks at approximately 2.8 and 3.5 Å, respectively. Sample M1Ca shows perhaps a hint of a second shell, but if one is present it is largely buried beneath the noise. The Ca K-edge (4038 eV) is near the practical lower limit of CHESS energies, making data collection more difficult and reducing the signal-to-noise ratio. (For this reason,

* $1\text{ Å}=10^{-1}$ nm

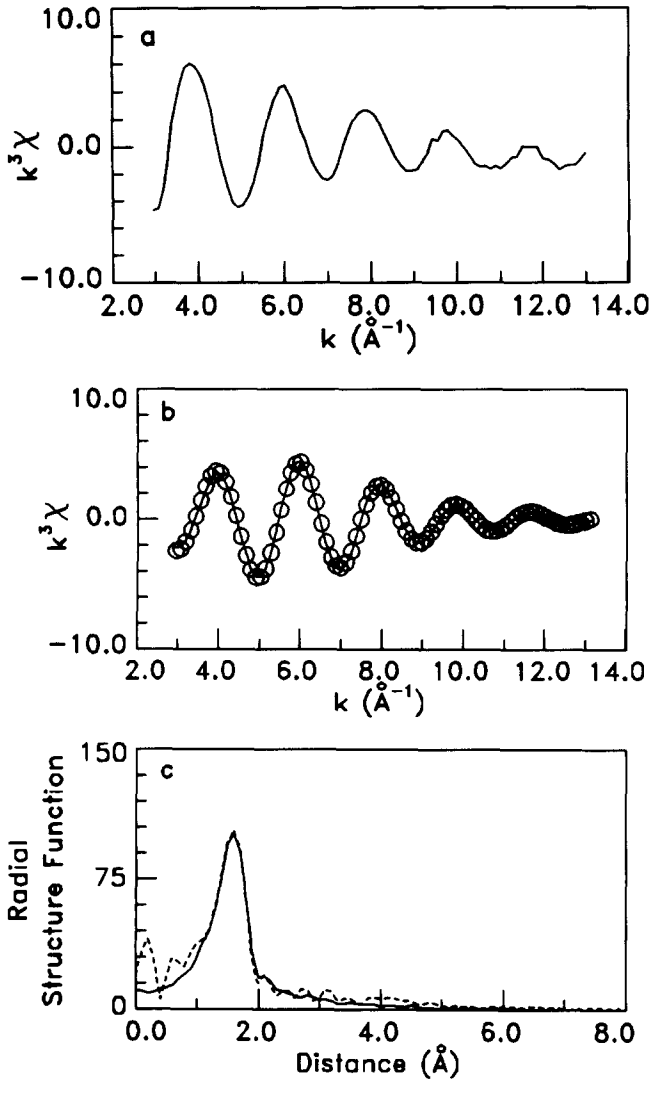

Figure 1 EXAFS data for M1Zn: (a) $k^3\chi$ *versus* k; (b) filtered $k^3\chi$ *versus* k (○) and fit (——); (c) radial structure function, transform of data in (a) (– – –) and fit (——)

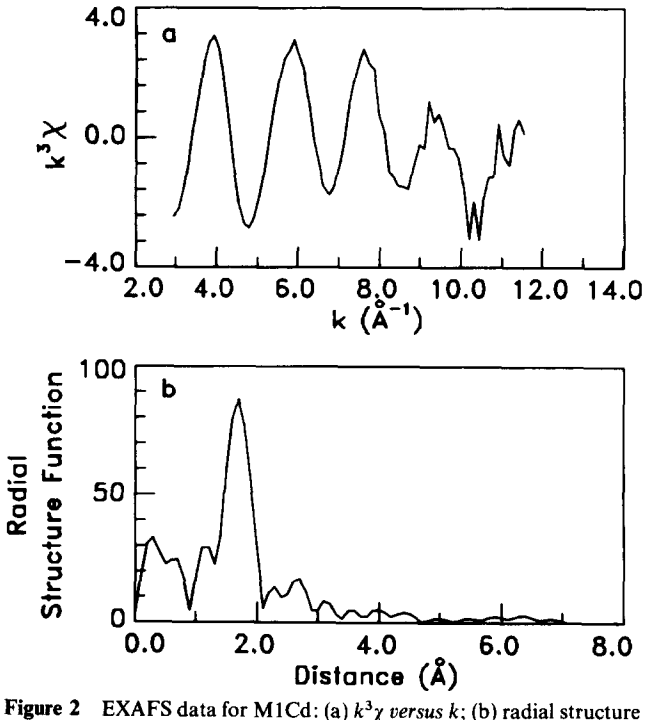

Figure 2 EXAFS data for M1Cd: (a) $k^3\chi$ *versus* k; (b) radial structure function

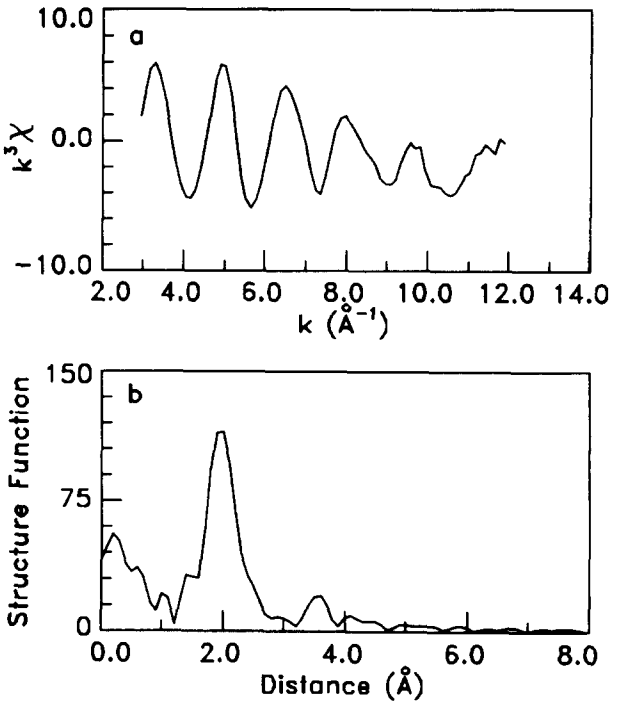

Figure 3 EXAFS data for M1Eu: (a) $k^3\chi$ *versus* k; (b) radial structure function

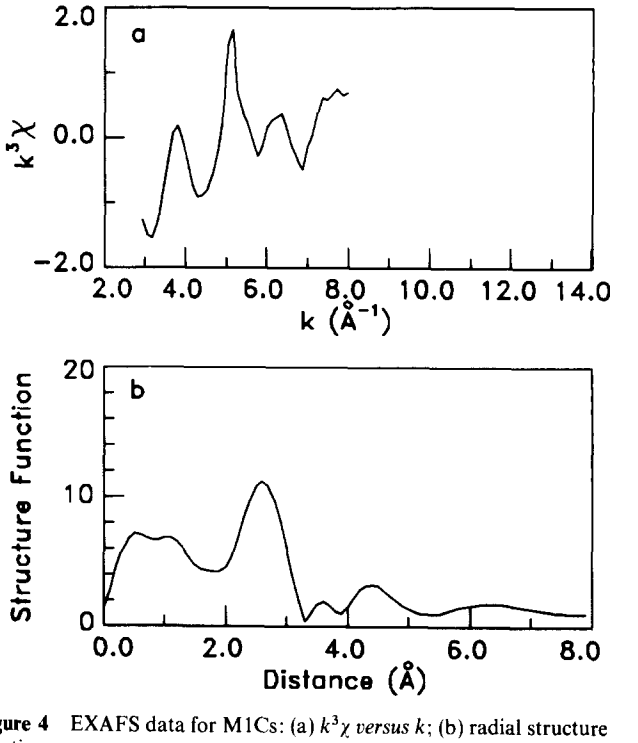

Figure 4 EXAFS data for M1Cs: (a) $k^3\chi$ *versus* k; (b) radial structure function

sample M1Na could not be examined, as the K-edge is at 1072 eV.) Sample M1Cd shows a strong first shell and perhaps a weak second shell, while M1Zn shows only a single shell. M1Cs shows what appears to be a weak shell near 2.8 Å, but the small peak height in the RSF shows that the structure is extremely disordered. This appears to be a general characteristic of large alkali metal cations. Previous investigations of Rb-neutralized perfluorosulphonated (Nafion) ionomers[6] also failed to show a good coordination structure, and recent investi-

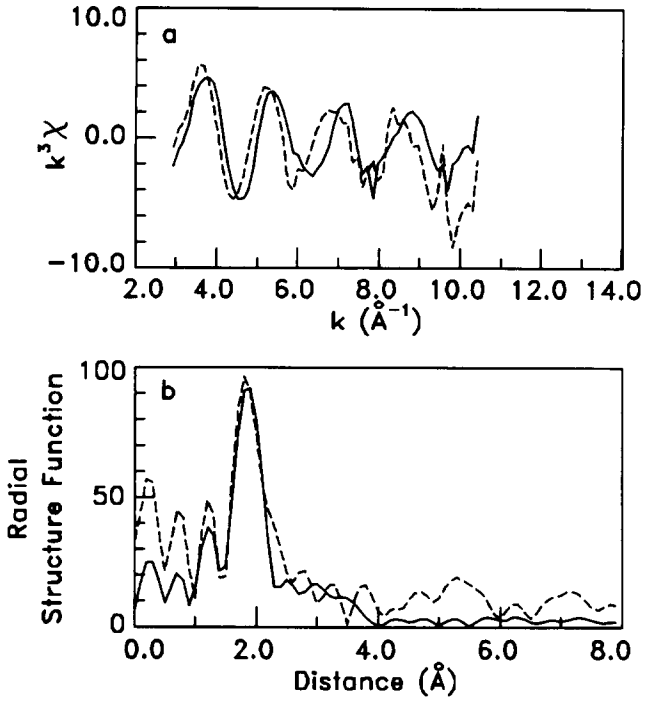

Figure 5 EXAFS data for M1Ca, dry (——) and hydrated (– – –): (a) $k^3\chi$ *versus* k; (b) radial structure function

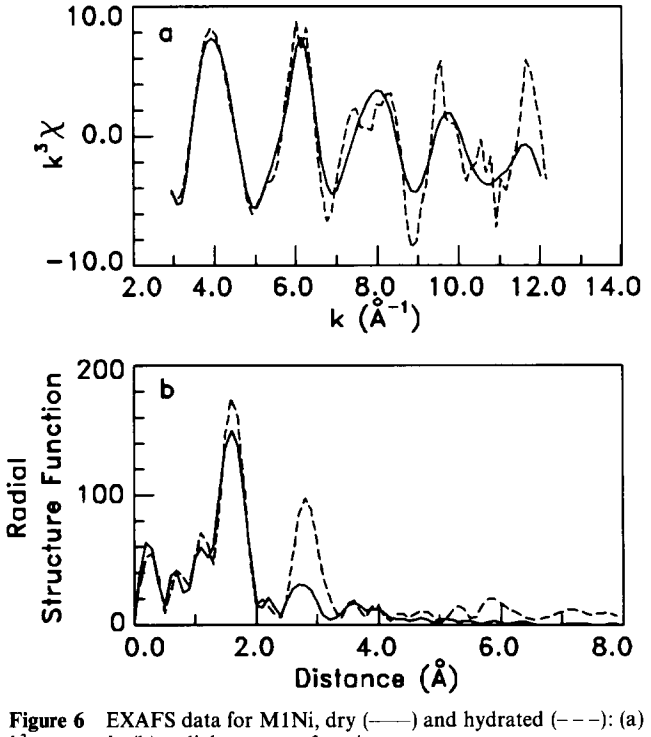

Figure 6 EXAFS data for M1Ni, dry (——) and hydrated (– – –): (a) $k^3\chi$ *versus* k; (b) radial structure function

gations of the living ends in Cs-initiated anionic polymerization showed no EXAFS oscillations at all[25]. Even model compounds such as CsF, while they do exhibit EXAFS, seem far more disordered than materials such as ZnO. In a previous paper[2], it was noted that the electron density difference between the aggregates and the matrix was unusually low in M1Cs, given the high atomic number of Cs. This is consistent with the EXAFS results, which indicate that the aggregates in M1Cs are disordered and loosely packed.

To quantify these results, the first shells of all samples (except M1Cs) as well as the second shell of M1Ni, were fitted to equation (1). The parameters obtained for the model compounds are listed in *Table 1*, and were used to construct the results for the ionomers listed in *Table 2*. To account approximately for small errors in the theoretical phase functions, the difference between the values of R_j determined by crystallography[26,27] and EXAFS were added to the values of R_j found for the ionomers. The correction was always small (<0.05 Å), except for CdO, where the EXAFS-measured Cd–O length was found to be 0.21 Å shorter than that determined by crystallography.

In all cases, the first shell was found to be due to oxygen atoms. These oxygens could arise from either water or sulphonate groups, although complete coordination by sulphonate is ruled out by the absence of a coordination shell due to sulphur. Such a structure has been observed previously by EXAFS for thoroughly dehydrated zinc-neutralized sulphonated polystyrene[7]. The presence of water in these materials is expected, based on the difficulty in drying sulphonated ionomers, as discussed previously[1]. Some of the values of N_1 are within 25% of 6, the value for the oxide model compound, although some are higher. This is likely to be due to the correlation between N and σ, as shown in equation (1); materials with large values of N also have large values of σ. As an example, examine *Figure 5*, where the dry and hydrated M1Ca samples are observed to be largely similar, especially in the amplitude of the $k^3\chi$ and RSF. The coordination numbers, however, are found to be 7.2 and 9.4, respectively, while the Debye–Waller factors σ_1 are found to be 0.070 and 0.088 Å, respectively. Fixing σ_1 for the hydrated sample at 0.070 Å led to a fit only slightly worse, with a value of N within 5% of that for the dry sample. This dilemma reflects the well-established fact

Table 1 Model compound parameters[a]

Compound	Shell number (j)	Shell element	R_j(Å)	$N_j\sigma_j$	N_j	λ_j(Å)
CaO	1	O	2.41	2.25	6	4.85
NiO	1	O	2.09	2.47	6	4.59
	2	Ni	2.95	5.95	12	8.36
ZnO	1	O	1.98	1.98	4	5.63
CdO	1	O	2.35	1.40	6	2.95
Eu_2O_3	1	O	2.32	3.10	6	7.03

[a] Distance values and coordination numbers determined from crystallography

Table 2 EXAFS structural parameters for the M1 series

Sample	Shell number (j)	Shell element	R_j(Å)	$N_j\gamma_j$	N_j	σ_j(Å)	Q(%)[a]
M1Ca-dry	1	O	2.37	2.75	7.3	0.070	3.83
M1Ca-hyd.	1	O	2.39	3.56	9.5	0.088	12.28
M1Ni-dry	1	O	2.08	3.36	8.3	0.075	1.83
	2	Ni	3.06	5.47		0.169	4.48
M1Ni-hyd.	1	O	2.09	3.03	7.5	0.058	6.45
	2	Ni	3.12	1.85	3.9	0.077	8.33
M1Zn	1	O	2.02	2.83	5.8	0.093	4.07
M1Cd	1	O	2.32	1.72	8.3	0.057	2.48
M1Eu	1	O	2.38	4.14	8.1	0.088	7.98

[a] The quality of fit, Q, is defined as the square root of the ratio of the sum of the squares of the residue to the sum of the squares of the data

that the strength of EXAFS is in determining atomic types and distances, but it is not as accurate in determining coordination numbers. Because of the similarities in first-shell distance of these materials to the model monoxides, as determined by crystallography (see *Table 1*), the first-shell coordination number for M1Ca, M1Ni, M1Cd and M1Eu is likely to be 6. The situation for M1Zn is more complicated, however, since Zn compounds are known to exhibit four-, five- or sixfold coordination. Fortunately, a study of model compounds by Pan *et al.*[6] has shown that there is a strong correlation between the Zn–O distance (which can be determined quite accurately by EXAFS) and the coordination number. The Zn–O distance here, 2.02 Å, falls squarely in the range found for fivefold coordination.

Consider next the hydrated samples. When these materials were swollen with water, they resembled weak gels, with essentially no mechanical strength, indicating that the ionic aggregates have ceased to be effective physical crosslinks. For M1Ca, hydration appears to have little effect on the local coordination structure, as shown in *Figure 5*. This is not too surprising, as most or all of the oxygen atoms in the first shell of the dry sample are assumed to be due to water. The results for the M1Ni sample are more surprising. Upon hydration, the second-shell peak grows substantially. Good fits to this peak were obtained, for both the dry and hydrated samples, using Ni atoms. (Sulphur and oxygen atom fits were also attempted, but did not yield good fits with physically reasonable parameters.) Such Ni–Ni distances have been observed previously in Nafion[3] and carboxy-telechelic polyisoprene[10] ionomers by EXAFS. The relatively small size of the peak in the dry sample makes fitting difficult, as shown by the anomalously large value of σ_2; the smaller the peak is, the more its shape is distorted by background noise. Therefore, the second-shell coordination number in the dry sample cannot be determined accurately. For the hydrated sample, a coordination number of approximately 4 is obtained, compared to 12 for NiO. This indicates a fairly densely packed structure, which is surprising for a hydrated material. However, dimers of Mo(IV) have been observed in acidic solution by EXAFS[28], and structures similar to that suggested here have been found in iron-neutralized Nafion[8]. The results can be rationalized by assuming that the structure is similar to the Mo(IV) dimers – that is, bridged by oxo or hydroxyl groups – but with a branched structure rather than simple dimers. It may be that the cations in the dry state are coordinated by a mixture of water and sulphonate groups, which prevents a highly ordered second shell from developing. In the hydrated state, the sulphonate groups are displaced, leading to the structure postulated above. Still, the enhancement of the second shell with hydration is a surprising result.

Returning to the dry samples, the first-shell coordination is similar for all. It is interesting to compare the presence or absence of a second shell with the tensile properties, as was done previously for the telechelic polyisoprenes[10]. For the M1 series, a good parameter to use for comparison is the elongation at the onset of stress crystallization, which may be approximated as the minimum in the Mooney–Rivlin plots, α_c, as shown previously[1]. If ion hopping is prevalent in a material, relaxation of the chains will delay the onset of stress crystallization. Therefore, α_c should be inversely related to the aggregate cohesiveness. For this series of materials[1], α_c was found to increase in the order M1Ni < M1Eu < M1Ca < M1Cd < M1Zn < M1Cs. The same ordering is observed in the strength of the second-shell peak by EXAFS here: M1Ni and MiEu have clear second-shell peaks in their RSFs; M1Ca and M1Cd may or may not have weak secondshell peaks; the M1Zn RSF clearly has only a single peak; and the M1Cs RSF has only one peak and a weak one at that. Therefore, it seems that in the dry samples, the postulate that aggregate cohesiveness controls the large-strain tensile properties is again verified.

CONCLUSIONS

A series of sulphonated polyurethanes based on PTMO-1000 and TDI, neutralized with Ca^{2+}, Ni^{2+}, Zn^{2+}, Cd^{2+}, Cs^{+}, and Eu^{3+}, was examined by EXAFS to determine the local coordination structure about the cation. The first shell in the M1Ca, M1Ni, M1Zn, and M1Eu materials was found to consist of six oxygen atoms, while M1Zn was coordinated by five oxygen atoms. M1Ni and M1Eu exhibited clear second coordination shells, M1Ca and M1Cd may have poorly ordered second shells, M1Zn has only a single shell, and M1Cs has only one shell of low order. The degree of local order correlates well with the elongation at the onset of strain hardening, as described in a previous publication on this same series of materials[1]. Therefore, in the dry state, the large-strain behaviour is controlled by the cohesiveness of the ionic aggregates and the resultant difficulty of ion hopping. Upon hydration, the materials become weak gels. The local structure in M1Ca appeared little affected by hydration, while for M1Ni the second-shell peak grew dramatically. This was attributed to the displacement of sulphonate groups from intimate contact with the cations and the development of a structure bridged exclusively by groups arising from water molecules.

ACKNOWLEDGEMENTS

The authors acknowledge partial support of this research by the US Department of Energy (DE-FG02-84-ER45111) and the Division of Materials Research of the National Science Foundation (DMR 86-03839). The help of the CHESS staff, Wilson Synchrotron Laboratory, Cornell University, in acquiring the EXAFS data is gratefully acknowledged. R.A.R. wishes to thank the Fannie and John Hertz Foundation for financial support while this work was completed.

REFERENCES

1 Ding, Y. S., Register, R. A., Yang, C.-z. and Cooper, S. L. *Polymer* 1989, **30**, 1204
2 Ding, Y. S., Register, R. A., Yang, C.-z. and Cooper, S. L. *Polymer* 1989, **30**, 1213
3 Pan, H. K., Yarusso, D. J., Knapp, G. S. and Cooper, S. L. *J. Polym. Sci., Polym. Phys. Edn.* 1983, **21**, 1389
4 Yarusso, D. J., Ding, Y. S., Pan, H. K. and Cooper, S. L. *J. Polym. Sci., Polym. Phys. Edn.* 1984, **22**, 2073
5 Pan, H. K., Yarusso, D. J., Knapp, G. S., Pinéri, M., Meagher, A., Coey, J. M. D. and Cooper, S. L. *J. Chem. Phys.* 1983, **79**, 4736
6 Pan, H. K., Knapp, G. S. and Cooper, S. L. *Colloid Polym. Sci.* 1984, **262**, 734
7 Ding, Y. S., Yarusso, D. J., Pan, H. K. and Cooper, S. L. *J. Appl. Phys.* 1984, **56**, 2396

8 Pan, H. K., Meagher, A., Pinéri, M., Knapp, G. S. and Cooper, S. L. *J. Chem. Phys.* 1985, **82**, 1529
9 Ding, Y. S., Register, R. A., Nagarjan, M. R., Pan, H. K. and Cooper, S. K. *J. Polym. Sci., Polym. Phys. Edn.* 1988, **26**, 289
10 Register, R. A., Foucart, M., Jérôme, R., Ding, Y. S. and Cooper, S. L. *Macromolecules* 1988, **21**, 2652
11 Jérôme, R., Vlaic, G. and Williams, C. E. *J. Phys. Lett.* 1983, **44**, L-717
12 Galland, D., Belakhovsky, M., Medrignac, F., Pinéri, M., Vlaic, G. and Jérôme, R. *Polymer* 1986, **27**, 883
13 Meagher, A., Coey, J. M. D., Belakhovsky, M., Pinéri, M., Jérôme, R., Vlaic, G., Williams, C. and Dang, N. V. *Polymer* 1986, **27**, 979
14 Ward, T. C. and Tobolsky, A. V. *J. Appl. Polym. Sci.* 1967, **11**, 2903
15 Sakamoto, K., MacKnight, W. J. and Porter, R. S. *J. Polym. Sci. A-2* 1970, **8**, 277
16 Hara, M., Eisenberg, A., Storey, R. F. and Kennedy, J. P. in 'Coulombic Interactions in Macromolecular Systems' (Eds A. Eisenberg and F. E. Bailey), *ACS Symp. Ser.* 1986, **302**
17 Wilson, F. C., Longworth, R. and Vaughan, D. J. *Polym. Prepr. Am. Chem. Soc. Div. Polym. Chem.* 1968, **9**, 505
18 Fitzgerald, J. J. and Weiss, R. A. in 'Coulombic Interactions in Macromolecular Systems' (Eds A. Eisenberg and F. E. Bailey), *ACS Symp. Ser.* 1986, **302**
19 Sayers, D. E., Stern, E. A. and Lytle, F. W. *Phys. Rev. Lett.* 1971, **27**, 1024
20 Stern, E. A., Sayers, D. E. and Lytle, F. W. *Phys. Rev. B* 1975, **11**, 4836
21 Lee, P. A., Citrin, P. H., Eisenberger, P. and Kincaid, B. M. *Rev. Mod. Phys.* 1981, **53**, 769
22 Teo, B. K. and Lee, P. A. *J. Am. Chem. Soc.* 1979, **101**, 2815
23 Lengler, B. and Eisenberger, P. *Phys. Rev. B* 1980, **22**, 4507
24 Stern, E. A. and Kim, K. *Phys. Rev. B* 1981, **23**, 781
25 Register, R. A., Cooper, S. L., Yoon, H. and Yu, H. Unpublished data, 1986
26 Donnay, J. D. H. and Ondik, H. M. (Eds) 'Crystal Data: Determinative Tables, Vol. II, 3rd. edn, National Bureau of Standards, Washington D.C., 1973
27 Abrahams, S. C. and Bernstein, J. L. *Acta Crystallogr.* 1969, **B25**, 1233
28 Cramer, S. P., Gray, H. B., Dori, Z. and Bino, A. *J. Am. Chem. Soc.* 1979, **101**, 2770
29 Pan, H. K. *Ph.D. thesis*, University of Wisconsin – Madison, 1983